

# Hydrodynamic extension of a two-component model for hadroproduction in heavy-ion collisions

A. A. Bylinkin,<sup>1,\*</sup>† N. S. Chernyavskaya,<sup>1,\*</sup>‡ and A. A. Rostovtsev<sup>2,§</sup>

<sup>1</sup>*Institute for Theoretical and Experimental Physics, ITEP, 117218 Moscow, Russia*

<sup>2</sup>*National Research Nuclear University Moscow Engineering Physics Institute, MEPhI, 115409 Moscow, Russia*

(Received 14 May 2014; published 9 July 2014)

The dependence of the spectral shape of produced charged hadrons on the size of a colliding system is discussed using a two-component model. As a result, the system-size hierarchy in spectral shape is observed. Next, a hydrodynamic extension of a two-component model for hadroproduction using recent theoretical calculations is suggested to describe the spectra of charged particles produced in heavy-ion collisions in the full range of transverse momenta  $p_T$ . Data from heavy-ion collisions measured at the Relativistic Heavy Ion Collider and the Large Hadron Collider are analyzed using the introduced approach and are combined in terms of energy density. The observed regularities might be explained by the formation of a quark-gluon plasma during the collision.

DOI: [10.1103/PhysRevC.90.018201](https://doi.org/10.1103/PhysRevC.90.018201)

PACS number(s): 25.75.Ld, 25.75.Dw, 25.75.Nq, 12.38.Mh

*Introduction.* Recently, a unified approach to describe charged particle production in high-energy collisions via two distinct mechanisms of hadroproduction has been proposed [1]. It was suggested that the charged particle spectra as a function of the particle's transverse momentum  $p_T$  could be approximated by a sum of exponential (Boltzmann-like) and power-law distributions:

$$\frac{d\sigma}{p_T dp_T} = A_e \exp(-E_{\text{Tkin}}/T_e) + \frac{A}{(1 + \frac{p_T^2}{T^2 \cdot N})^N}, \quad (1)$$

where  $E_{\text{Tkin}} = \sqrt{p_T^2 + M^2} - M$  with  $M$  equal to the produced hadron mass.  $A_e$ ,  $A$ ,  $T_e$ ,  $T$ ,  $N$  are the free parameters to be determined by a fit to the data.

According to this approach, the exponential part stands for the release of “thermalized” particles by the preexisting valence quarks and a quark-gluon cloud coupled to them inside the colliding baryon. The power-law term accounts for the fragmentation of mini-jets formed by the secondary partons (gluons) produced with a relatively large  $k_T$  at the first stage of the collision, which can be described within perturbative quantum chromo-dynamics (pQCD). From this qualitative picture of hadroproduction one can naively expect that the spectra of charged hadrons in  $\gamma\gamma$  collisions should be described by the power-law term alone due to the absence of “thermalized” quarks and gluons in the colliding systems. Such behavior has also been proven recently [2].

Thus, it is interesting to compare the shapes of charged particles produced in these two types of interactions ( $\gamma\gamma$  and  $pp$ ) with the more complex case of heavy-ion collisions.

*Hierarchy in hadroproduction dynamics.* Let us look at the recent data on lead-lead collisions measured by the ALICE Collaboration [3] in the range of transverse momentum  $p_T$  up

to 50 GeV. Figure 1 shows experimental data on  $\gamma\gamma$  [4],  $pp$  [5], and lead-lead [3] collisions fitted with the parametrization introduced (1). One can notice that this parametrization cannot describe the shape of the spectra in lead-lead collisions for the very high  $p_T$  values and an additional power-law term is needed:

$$\frac{d\sigma}{p_T dp_T} = A_e \exp(-E_{\text{Tkin}}/T_e) + \frac{A}{(1 + \frac{p_T^2}{T^2 \cdot N})^N} + \frac{A_1}{(1 + \frac{p_T^2}{T_1^2 \cdot N_1})^{N_1}}. \quad (2)$$

Note that an additional power-law term in lead-lead collisions might be explained by the peculiar shape of the nuclear modification factor  $R_{AA}$ . Figure 2 shows  $R_{AA}$  for lead-lead collisions measured by the ALICE Collaboration [3] together with the lines showing contributions from the three terms of Eq. (2) independently, each of them divided over the spectrum in  $pp$  collisions measured at the same center-of-mass (c.m.) energy [5]. One can notice that each of these terms contributes to different regions of the transverse momentum  $p_T$ . The observed behavior might be explained by the following picture of hadroproduction in heavy-ion collisions:

- (i) The bulk of low- $p_T$  particles originates from the “quark-gluon soup” formed in the heavy-ion collision and has an exponential  $p_T$  distribution, as shown by the red dashed line in Figs. 1 and 2.
- (ii) The high- $p_T$  tail (shown by the green solid line in Figs. 1 and 2) accounts for the mini-jets that pass through the nuclei, a process that can be described in pQCD [6]. When these jets hadronize into final-state particles *outside* the nuclei, we get the same power-law term parameter  $N$  as in  $pp$  collisions [Figs. 1(b) and 1(c)], resulting in a constant suppression ( $R_{AA}$ ) of high- $p_T$  ( $>20$  GeV) particles (Fig. 2). Note that while passing through the nuclei these jets should lose about  $\frac{dE}{dz} \cdot R_A \sim 7$  GeV [6], where  $R_A$  is the radius of the nuclei. Therefore, hadrons with  $p_T < 7$  GeV produced from these jets will be largely suppressed, as seen in Fig. 2.

\*Also at Moscow Institute of Physics and Technology, MIPT, 9 Institutskiy per., Dolgoprudny, Moscow Region, 141700, Russian Federation.

†alexander.bylinkin@desy.de

‡nadezda.chernyavskaya@desy.de

§rostov@itep.ru

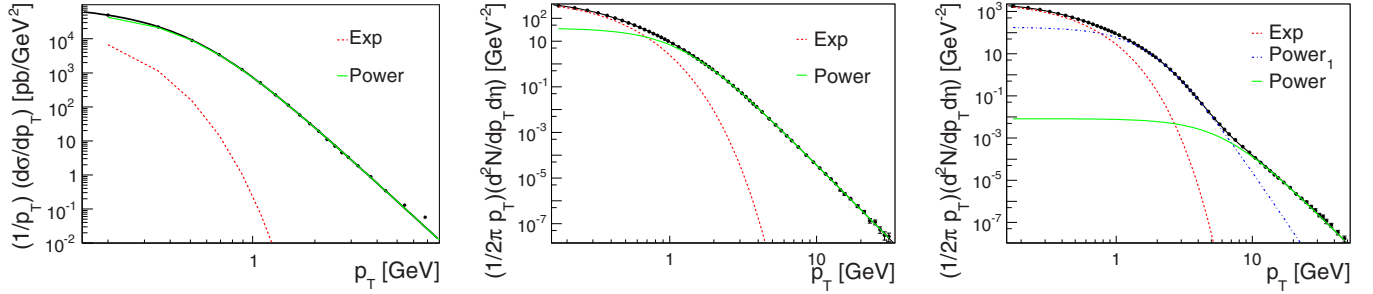


FIG. 1. (Color online) Charged particle spectra in  $\gamma\gamma$  [4] (a),  $pp$  [5] (b), and central lead-lead collisions [3] (c) fitted to the function (2); the red (dashed) line shows the exponential term and the green (solid) and blue (dash-dot) lines show the two power-law terms.

- (iii) On the other hand, mini-jet fragmentation into final-state hadrons can also occur before the jet leaves the nuclei volume. The produced particles have to wade out through the nuclei, being affected by multiple rescatterings, and thus their distribution (blue dash-dot line in Figs. 1 and 2) becomes closer to the exponent, resulting in higher values of  $N_1$  and  $T_1$  of the power-law term, and dominates the mid- $p_T$  region. This process cannot be described in pQCD, however.

Now one can notice the hierarchy in hadroproduction dynamics by complexity (number of involved partons or initial size) of the colliding system:

- (i)  $\gamma\gamma$  collision: This is a pointlike interaction that can be described in terms of pQCD and thus needs a power-law term only in its spectrum.
- (ii) Baryon-baryon collision: In addition to the mini-jet fragmentation of the virtual partons an exponential term standing for the release of thermalized particles due to preexisting quarks and gluons is added. Therefore, one gets a sum of exponential and power-law terms to describe the spectra in  $pp$  collisions.
- (iii) Heavy-ion collision: Owing to the quenching of charged hadrons inside the nuclei the power-law term splits into two distributions with different parameters

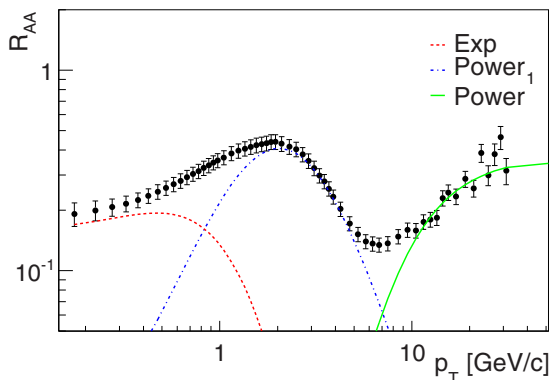


FIG. 2. (Color online) Nuclear modification factor  $R_{AA}$  measured for central lead-lead collisions [3] shown together with the terms of (2) independently divided over the fit (1) of the  $pp$  data at the same c.m.s energy; the red (dashed) line shows the exponential term and the green (solid) and blue (dash-dot) lines show the two power-law terms.

(the second closer to the exponent). Therefore, we need a sum of exponential and two power-law terms to describe the spectra.

*Hydrodynamic extension of the model.* Though the parametrization using an exponential and two power-law terms (2) gives a rather perfect description of the experimental data [3] [Fig. 1(c)], it is known that Boltzmann thermodynamics is not applicable for heavy-ion collisions. When a large colliding system is formed, one should also take the effects of the “collective motion” into account [7]. Thus, in heavy-ion collisions multiparticle production is usually considered in terms of relativistic hydrodynamics, contrary to the widely used thermodynamic approaches [8,9] for  $pp$ ,  $\gamma p$ , and  $\gamma\gamma$  collisions. Therefore, this suggests modifying the introduced approach (1) using recent theoretical calculations [7].

The idea of a hydrodynamic approach is that the thermalized system expands collectively in the longitudinal direction, generating the transverse flow by the high pressure in the colliding system. According to this approach the radiation of thermalized particles can be parametrized by the following formula:

$$\frac{dn}{p_T dp_T} \propto \int_0^R r dr m_T I_0 \left( \frac{p_T \sinh \rho}{T_e} \right) K_1 \left( \frac{m_T \cosh \rho}{T_e} \right), \quad (3)$$

where  $\rho = \tanh^{-1} \beta_r$  and  $\beta_r(r) = \beta_s(\frac{r}{R})$ , with  $\beta_s$  standing for the surface velocity. In this analysis we take  $\beta_s = 0.5c$ , which is consistent with previous observations [7]. Thus, one has to substitute the exponential term in (1) by (3).

Note that the power-law term in (1) stands for the pointlike pQCD interactions that occur in the early stage of the collision, with the hadrons produced from the mini-jet fragmentation leaving the interaction area before reaching thermal equilibrium. Therefore, we assume this term to be considered without taking the “collective motion” into account.

Now one can use this hydrodynamic approach to fit the recent experimental data on lead-lead collisions measured by the Alice Collaboration [3] at  $\sqrt{s} = 2.76$  TeV.

These data are shown in Fig. 3 together with the fit

$$\frac{dn}{p_T dp_T} = A_e \cdot \int_0^R r dr m_T I_0 \left( \frac{p_T \sinh \rho}{T_e} \right) K_1 \left( \frac{m_T \cosh \rho}{T_e} \right) + \frac{A}{(1 + \frac{p_T^2}{T^2 \cdot N})^N} + \frac{A_1}{(1 + \frac{p_T^2}{T_1^2 \cdot N_1})^{N_1}}. \quad (4)$$

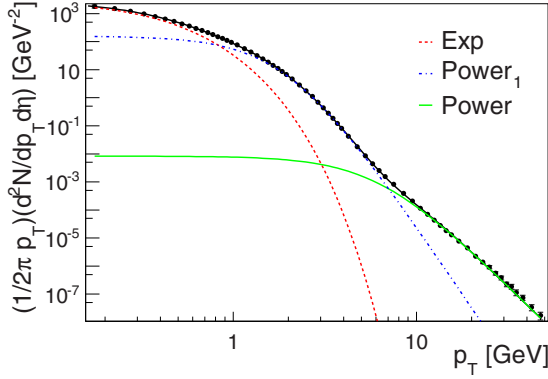


FIG. 3. (Color online) Central lead-lead collisions [3] fitted with (4); the red (dashed) line shows the hydrodynamic term and the green (solid) and blue (dash-dot) lines show the two power-law terms.

Note that the proposed hydrodynamic extension (4) of (1) only slightly modifies the description of the experimental data and still two power-law terms are needed. However, the values of the parameter  $T_e$  extracted from parametrizations (2) and (4) differ significantly (Fig. 4).

*Freeze-out temperature and combination of Relativistic Heavy Ion Collider and Large Hadron Collider data.* The introduced approach (4) allows us to extract the thermalized production [described by function (3)] of charged hadrons from the whole statistical ensemble. In this Brief Report we propose to study the variations of the temperature-like parameter  $T_e$  in (3) with the centrality and the c.m. energy in heavy-ion collisions. Therefore, it is interesting to consider the experimental data measured at the Relativistic Heavy Ion Collider (RHIC) and the Large Hadron Collider (LHC) together.

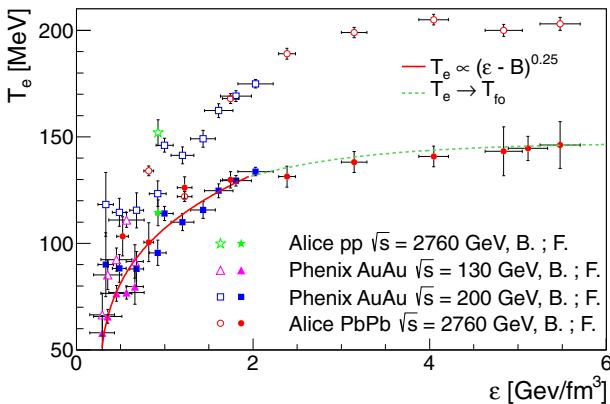


FIG. 4. (Color online) Temperature of the final-state hadrons coming from the thermalized part of the spectra in heavy-ion collisions as a function of energy density. Full points show the results extracted from the fit by taking into account the collective flow (4) (marked with F. in the legend); open points show the results when using a fit with the Boltzmann exponent (2) (marked with B in the legend). The solid line stands for the  $T_e \propto (\epsilon - B)^{0.25}$  fit and the dashed line shows  $T_e \rightarrow \text{const.}$  behavior.

Since the center-of-mass energies per nucleon in these experiments are varied by a factor of  $\approx 20$ , a unified approach considering the energy density is suggested. The energy density in heavy-ion interactions is known to depend not only on the center-of-mass energy but also on the centrality of the collision. Hence, while the maximum energy densities that can be reached at RHIC and at LHC differ significantly, the energy density in central collisions at RHIC might be of the same order as that in peripheral collisions at LHC.

In this paper we consider the experimental data measured in Au-Au collisions at  $\sqrt{s} = 200$  GeV/N and  $\sqrt{s} = 130$  GeV/N by the PHENIX Collaboration [10,11] and in Pb-Pb collisions at  $\sqrt{s} = 2.76$  TeV/N by the ALICE Collaboration [3].

The energy density  $\epsilon$  for central collisions can be determined from the experimental data by using the formula [12]

$$\frac{dE_T}{d\eta}(\eta \sim 0) = \pi R^2 \epsilon_f \tau_0, \quad (5)$$

where  $\epsilon_f$  is the energy density averaged over the transverse area and  $R$  is the nuclear radius.

However, for noncentral collisions it is more convenient to estimate it using a simple parametrization [12]:

$$\epsilon = \epsilon_0 \left( \frac{s}{s_0} \right)^{\alpha/2} N_{\text{coll}}^\beta, \quad (6)$$

with  $\epsilon_0$  calculated for the most central collisions,  $\alpha \approx 0.3$  [13],  $\beta \approx 0.5$  [14], and  $\sqrt{s_0} = 200$  GeV [12]. Here the second factor is responsible for the incident energy dependence,  $\sqrt{s}$  is the c.m. collision energy, and the third one shows the dependence on the number of binary parton-parton collisions,  $N_{\text{coll}}$ , which is related to the centrality of the collision. Note that in this analysis  $\epsilon_0$  turned out to be the same for PHENIX and ALICE data, thus confirming the  $\alpha = 0.3$  value proposed in [13].

Having calculated the energy density  $\epsilon$  using the formula (6), one can plot the temperature  $T_e$  extracted from (4) as a function of it, as shown with full points in Fig. 4. First, as was expected, the energy density obtained in central collisions at RHIC is similar to those in peripheral collisions at LHC, and, remarkably, a smooth transition in the  $T_e$  values between these three measurements is also observed. Note that, as one could naively expect, the value of  $T_e$  [as well as  $N$  and  $T$  of the power-law term in (4)] for peripheral lead-lead collisions turns out to be practically identical with that obtained for  $pp$  collisions at the same c.m. energy [5].

Next, one can notice rather interesting behavior of the temperature  $T_e$  as a function of energy density ( $\epsilon \propto T_e^4 + B$ ), which is in a good agreement with the bag model [15], with  $B = 0.25$  GeV/fm<sup>3</sup>, as determined from the fit in Fig. 4. Another remarkable observation about the temperature  $T_e$  of the final-state particles is that for high energy densities it reaches a certain limit. This might be explained from a quark-gluon plasma (QGP) theory that considers the phase transition temperature  $T_c$  from the QGP to final-state hadrons: the expanding system cools down until it reaches the freeze-out stage; thus, the temperature of the final-state particles should always be below  $T_c$ . Indeed, for high values of  $\epsilon$  one can notice that the observed freeze-out temperature is  $T_{fo} \approx 145$  MeV, and (as one can expect) this is slightly

below the critical temperature  $T_c \sim 155\text{--}160$  MeV for QGP obtained in different calculations [16,17]. Note that when using the approximation without taking the collective flow into account [Eq. (2) with the Boltzmann exponent] one gets much higher values of the freeze-out temperature (open points in Fig. 4) than one might expect:  $T_{fo}^{\text{Boltzmann}} \approx 205$  MeV. This observation supports the idea of using the extension of the model with collective flow instead of the Boltzmann thermodynamics to describe hadroproduction in heavy-ion collisions.

*Conclusion.* The spectra of charged hadron production in heavy-ion collisions have been compared with those measured in  $pp$  and  $\gamma\gamma$  interactions using the recently introduced two-component model. The observed hierarchy on the size of the colliding system has been discussed and the qualitative

picture for hadroproduction in heavy-ion collisions explaining the peculiar shape of nuclear modification factor,  $R_{AA}$ , has been introduced. Next, a hydrodynamic extension of this parametrization accounting for the collective motion in heavy-ion collisions was suggested. This approach allowed us to extract the thermalized production of charged hadrons from the whole statistical ensemble and to study it separately. Thus, the variations of the temperature of the final-state hadrons coming from the thermalized part of the spectra have been studied as a function of energy density using both RHIC and LHC data and the behavior that might be explained in terms of QGP formation has been observed.

*Acknowledgment.* The authors thank Professor Mikhail Ryskin for fruitful discussions and the help he provided during the preparation of this paper.

- 
- [1] A. A. Bylinkin and A. A. Rostovtsev, *Phys. Atom. Nucl.* **75**, 999 (2012) [*Yad. Fiz.* **75**, 1060 (2012)]; [arXiv:1008.0332](#) [hep-ph]; [arXiv:1404.7302](#) [hep-ph].
- [2] A. A. Bylinkin and A. A. Rostovtsev, *Eur. Phys. J. C* **72**, 1961 (2012).
- [3] B. Abelev *et al.* (ALICE Collaboration), *Phys. Lett. B* **720**, 52 (2013).
- [4] G. Abbiendi *et al.* (OPAL Collaboration), *Phys. Lett. B* **651**, 922007.
- [5] B. B. Abelev *et al.* (ALICE Collaboration), *Eur. Phys. J. C* **73**, 2662 (2013).
- [6] X.-N. Wang, *Phys. Rep.* **280**, 287 (1997).
- [7] E. Schnedermann, J. Sollfrank, and U. W. Heinz, *Phys. Rev. C* **48**, 2462 (1993).
- [8] C. Tsallis, *J. Stat. Phys.* **52**, 479 (1988); *Braz. J. Phys.* **29**, 1 (1999).
- [9] R. Hagedorn, *Riv. Nuovo Cim.* **6N10**, 1 (1984).
- [10] S. S. Adler *et al.* (PHENIX Collaboration), *Phys. Rev. C* **69**, 034909 (2004).
- [11] K. Adcox *et al.* (PHENIX Collaboration), *Phys. Rev. C* **69**, 024904 (2004).
- [12] I. N. Mishustin and J. I. Kapusta, *Phys. Rev. Lett.* **88**, 112501 (2002).
- [13] D. Kharzeev and E. Levin, *Phys. Lett. B* **523**, 79 (2001).
- [14] M. A. Braun, F. del Moral, and C. Pajares, *Phys. Rev. C* **65**, 024907 (2002).
- [15] A. Chodos, R. L. Jaffe, K. Johnson, C. B. Thorn, and V. F. Weisskopf, *Phys. Rev. D* **9**, 3471 (1974).
- [16] F. Karsch, K. Redlich, and A. Tawfik, *Eur. Phys. J. C* **29**, 549 (2003).
- [17] A. Majumder and B. Muller, *Phys. Rev. Lett.* **105**, 252002 (2010).